Available online at www.sciencedirect.com
SCIENCE DIRECT®
Polyhedron 22 (2003) 3171–3179
POLYHEDRON
www.elsevier.com/locate/poly

The characterisation of lead fatty acid soaps in 'protrusions' in aged traditional oil paint

M. John Plater [a,*], Ben De Silva [a], Thomas Gelbrich [b], Michael B. Hursthouse [b], Catherine L. Higgitt [c], David R. Saunders [c]

[a] Department of Chemistry, University of Aberdeen, Meston Walk, Aberdeen, Scotland AB24 3UE, UK
[b] Department of Chemistry, University of Southampton, Highfield, Southampton SO17 1BJ, UK
[c] Scientific Department, The National Gallery, Trafalgar Square, London WC2N 5DN, UK

Received 19 May 2003; accepted 8 July 2003

Abstract

Lead(II) carboxylate soaps of two fatty acids, palmitic ($C_{15}H_{31}COOH$) and stearic acids ($C_{17}H_{35}COOH$), and a dicarboxylic acid, azelaic acid ($HOOCC_7H_{14}COOH$), have been synthesised and characterised by FTIR spectroscopy. These acids are all encountered in aged traditional oil paint, the azelaic acid resulting from the oxidative degradation of unsaturated fatty acids in the oil. Lead(II) azelate synthesised by hydrothermal methods was characterised by single crystal structure determination. This has a 3D polymeric structure with lead(II) ions linked by carboxylate bridges to form an infinite stack of $(PbO_4)_n$ units. These layers are connected to adjacent layers by an infinite number of parallel $C(CH_2)_7C$ chains arranged perpendicularly to the stacks. The lead(II) ions display an unusual 7-fold coordination. The first direct evidence that the 'protrusions' encountered in aged traditional lead-containing oil paints contain lead soaps is reported. Their mechanism of formation is discussed.

Keywords: Lead soaps; Hydrothermal; Palmitic acid; Stearic acid; Red lead; Lead-tin yellow

1. Introduction

Inclusions in paint samples from Old Master paintings have recently been found to contain lead(II) carboxylate salts (fatty acid soaps) [1,2]. These inclusions, which can sometimes be seen as lumps or protrusions on the paint surface, are believed to have formed from the reaction of certain lead-based pigments such as red lead (Pb_3O_4) and lead-tin yellow 'type I' (Pb_2SnO_4) with the fatty acid moieties of the triglycerides in traditional drying oils. Similar long chain fatty acid soaps of lead, copper and zinc have also been found as degradation products on the surfaces of metallic cultural artefacts, as a result of surface treatments or contact with organic components such as leather [3].

The results presented in this study are not only of relevance to the study of cultural artefacts and oil paintings but increase the understanding of a group of compounds of considerable commercial importance: long chain carboxylate soaps have been used as lubricants, driers in paints and inks, catalysts, polymer stabilisers, fuel additives, germicides and in corrosion inhibition [4–6]. Further, lamellar transition metal soaps, and dicarboxylate soaps in particular, are being investigated to assist in the design of novel magnetic materials [7,8].

GC-MS analysis of the total fatty acid content of the inclusions from within old paint layers has revealed that just three acids comprise the bulk of the monomeric content [1,9]. These acids are the stable saturated C_{16} and C_{18} straight-chain monocarboxylic fatty acids, palmitic and stearic acids, and the saturated C_9 dicarboxylic acid, azelaic acid. Azelaic acid is an oxidative degradation product of the polyunsaturated C_{18} fatty acids found in drying oils that are responsible for

* Corresponding author. Tel.: +44-1224-272-943; fax: +44-1224-272-921.
E-mail addresses: m.j.plater@abdn.ac.uk (M.J. Plater), catherine.higgitt@ng-london.org.uk (C.L. Higgitt).

0277-5387/$ - see front matter © 2003 Elsevier Ltd. All rights reserved.
doi:10.1016/S0277-5387(03)00461-3

the curing behaviour of such oils [9]. Oxidative cleavage of the double bond nearest the acid group [$-CH=CH(CH_2)_7CO_2H$] leads to azelaic acid. This structural feature occurs for all the unsaturated fatty acids and thus explains why azelaic acid is the main degradation product. The rapid cross-linking of the polyunsaturated fatty acids during drying, and the oxidative degradation reactions that occur, accounts for the absence of monomeric polyunsaturated fatty acids in the samples examined [9].

While lead carboxylates with a variety of ligand types have been reported in the crystallographic literature, rather fewer examples of salts of simple mono- or dibasic carboxylic acids are known [10]. The metal salts of long chain fatty acids have received even less attention, perhaps because of the difficulties in isolating pure single crystals of metal soaps [3,4,7,8,11]. The structural information that is available is based on X-ray powder diffraction, NMR and spectroscopic studies [4,12,13]. Therefore, to assist with studies of the inclusions present in authentic paint samples, standards of the lead soaps of palmitic, stearic and azelaic acid, were prepared and characterised. The majority of lead(II) carboxylates that have been characterised by crystallographic means have been shown to have polymeric structures [10]. Pb(II) shows a rich coordination chemistry, forming a range of polymeric and polynuclear complexes, displaying interesting structural and coordination features [10,14]. The polymeric structures contain bridging carboxylate oxygen atoms, with polybasic carboxylates offering even greater polymer formation possibilities. Hydrothermal synthesis has proved an extremely useful technique for the preparation of crystals of cross-linked polymeric solids suitable for characterisation by single crystal X-ray diffraction and this method was therefore adopted in the preparation of lead(II) azelate [10].

Other studies of the inclusions in paint samples using a variety of infrared and mass spectrometric techniques have demonstrated the presence of lead fatty acid soaps [2,3], but this study provides the first direct evidence for the presence of a mixture of lead palmitate and stearate in such inclusions, and the absence of lead azelate or other lead carboxylates.

2. Experimental

The equipment used for hydrothermal synthesis was as previously described [15]. Infrared spectra were recorded on KBr discs using a ATI Mattson Genesis series FTIR spectrometer or were obtained using a Nicolet 710 Series FTIR spectrometer using KBr pellets. Infrared spectra for authentic paint samples were acquired using a Nicolet 710 Series FTIR spectrometer with NicPlan infrared microscope, fitted with a MCT Type A detector. The samples were placed in a Spectra-Tech micro compression diamond cell and examined in transmission mode. To select the area to be examined, apertures are used to mask out the area of interest. The use of redundant apertures in the NicPlan microscope allows a lower sample size limit of ca. 10 μm [16]. The C, H, Pb microanalyses were performed by Butterworth Laboratories. Melting points (mp) were determined in open tubes with a Gallenkamp apparatus and are uncorrected. Paint samples mounted as cross-sections in polyester resin blocks were examined using a Cambridge Instruments S200 Scanning Electron Microscope fitted with an Oxford Instruments AN10000 Energy Dispersive X-ray Analyser. Samples for GC-MS analysis were treated with a 5% methanolic solution of (*m*-trifluoromethylphenyl)trimethlyammonium hydroxide [17]. This reagent hydrolyses glyceride linkages and forms the quaternary ammonium salts of carboxylic acids. Thermal degradation of these salts in the heated injector port of the GC results in in situ methylation of the carboxylic acids. GC-MS analysis was carried out using a HT5 quartz capillary column, programmed from 70 to 300 °C at 10 °C/min. with He carrier gas and splitless injection (injector temperature 250 °C) on a HP5890 GC. The GC is coupled to a VG Trio 2000 quadrupole mass spectrometer, scanning in EI^+ mode with source temperature of 210 °C.

2.1. Synthesis of monocarboxylate soaps

2.1.1. Method 1: Ambient synthesis of lead stearate and palmitate

The lead(II) soaps of stearic and palmitic acid were prepared using a modification of the precipitation method [4,18]. Aqueous solutions of $Pb(OAc)_2 \cdot 3H_2O$ or $Pb(NO_3)_2$ were prepared and mixed with methanolic solutions of the appropriate fatty acid in an approximate 1:2 stoichiometry. On mixing a white precipitate of the insoluble lead soap immediately formed. Excess starting material and the acid by-product were removed by washing the precipitate with water or EtOH.

Lead(II) palmitate. IR (KBr, cm^{-1}): 2955w, 2918vs, 2871sh, 2849vs, 1541s, 1513s, 1473m, 1462m, 1419m, 1407sh, 1349w, 1333w, 1315w, 1295w, 1274w, 1253w, 1232w, 1210w, 1189w, 1116vw, 1102vw, 1012vw, 930w, 892vw, 851vw, 816vw, 781vw, 731w, 719w, 706vw and 697vw; mp 112 °C (lit. 112.3) [19].

Lead(II) stearate. IR (KBr, cm^{-1}): 2955w, 2918vs, 2871w, 2849vs, 1540s, 1513s, 1473m, 1462m, 1419m, 1402sh, 1347w, 1333w, 1318w, 1299w, 1281w, 1263w, 1244w, 1225w, 1206w, 1187w, 1116vw, 1104vw, 1072vw, 1031vw, 930w, 812vw, 760vw, 731w, 719w and 706w; mp 115.5 °C (lit. 115.7) [19].

2.1.2. Method 2: Hydrothermal synthesis

Lead palmitate. Palmitic acid (200 mg, 0.779 mmol) and $Pb(OAc)_2 \cdot 3H_2O$ (148 mg, 0.390 mmol) in H_2O

(10 ml) were placed in a Parr 23 ml teflon lined bomb. This was heated up to 220 °C over 3 h, held at this temperature for 3 h, then cooled to room temperature over a further 3 h. Opaque light brown crystals (194 mg, 69%) were collected, washed with MeOH and dried in a desiccator for 24 h. *Anal.* Calc. For $C_{32}H_{62}O_4Pb$: C, 53.5; H, 8.7. Found: C, 53.7; H, 8.6%. IR as above.

Lead stearate. Stearic acid (200 mg, 0.703 mmol) and $Pb(OAc)_2 \cdot 3H_2O$ (133 mg, 0.351 mmol) in H_2O (10 ml) were placed in a Parr 23 ml teflon lined bomb. This was heated up to 220 °C over 3 h, held at this temperature for 3 h, then cooled to room temperature over a further 3 h. Opaque light brown crystals (188 mg, 69%) were collected, washed with MeOH and dried in a desiccator for 24 h. *Anal.* Calc. For $C_{36}H_{70}O_4Pb$: C, 55.85; H, 9.1. Found: C, 55.8; H, 9.0%. IR as above.

2.2. Synthesis of lead azelate

2.2.1. Method 1: Ambient synthesis

$Pb(NO_3)_2$ (1.68 g, 5.07 mmol) was dissolved in a mixture of EtOH (25 ml), MeOH (10 ml) and H_2O (25 ml). A solution of azelaic acid (0.95 g, 5.05 mmol) in EtOH (25 ml) was then prepared. Both solutions were placed in an ultrasonic bath until complete dissolution had been achieved and then warmed to 40 °C in a water bath. After mixing the resulting solution was covered with a watch glass and left in the water bath to return to ambient temperature (ca. 22 °C). After a further 12 h at ambient temperature, the supernatant liquid was pipetted off and the colourless crystals that remained were washed three times with 10 ml aliquots of H_2O:EtOH (1:4 v/v). Finally, the crystals were washed with EtOH (10 ml) and air dried. IR spectroscopy confirmed that the crystals were free of excess starting material or by-products. *Anal.* Calc. For $C_9H_{14}O_4Pb$: C, 27.48; H, 3.59; Pb, 52.67. Found: C, 26.53; H, 3.26; Pb, 52.67%. IR (KBr, cm^{-1}): 2959sh, 2931s, 2914sh, 2854s, 1517vs, 1444vs, 1403vs, 1364sh, 1341m, 1315w, 1283 and 1271m, 1245m, 1209w, 1118m, 1103m, 1094m, 988w, 941m, 827w, 769m, 722m and 665m; mp $>$ 240 °C (decomp.).

2.2.2. Method 2: Hydrothermal synthesis

Azelaic acid (200 mg, 1.063 mmol) and $Pb(OAc)_2 \cdot 3H_2O$ (403 mg, 1.063 mmol) in H_2O (10 ml) were placed in a Parr 23 ml teflon lined bomb. This was heated up to 220 °C over 3 h, held at this temperature for 3 h, then cooled to room temperature over a further 3 h. Opaque light brown crystals (320 mg, 76%) were collected, washed with H_2O and air dried. *Anal.* Calc. For $C_9H_{14}O_4Pb$: C, 27.5; H, 3.6. Found: C, 27.4; H, 3.45%. IR as above.

2.3. GC-MS analysis

20 independent samples of paint containing inclusions were collected from paintings ranging in date from the 14th to the 18th centuries, and analysed for the total fatty acid content [1]. This revealed the presence of palmitic, stearic and azelaic acids.

2.4. X-ray structure determination

Intensity data were recorded at 120 K, using a Nonius Kappa CCD area-detector diffractometer mounted at the window of a rotating anode FR591 generator with a molybdenum anode (0.71073 Å). φ and ω scans (2° increments) were carried out to fill the Ewald sphere. Data collection and processing were carried out using the programs DIRAX and COLLECT and an empirical absorption correction was applied using SORTAV [20–22]. The structure was solved by direct methods and refined on F^2 by full-matrix least-squares refinements [23,24]. All hydrogen atoms were included in the refinement in calculated positions using a riding model. An alternative refinement was carried out in the space group $P2_1$. Here, the mirror symmetry of the structure was still present, and it was decided to proceed in $P2_1/m$.

3. Results and discussion

3.1. Analysis of protrusions in paint samples

Attempts to determine the composition of the protrusions encountered in a wide variety of oil paintings ranging in date from the 13th to 18th centuries are hampered by the small size of the protrusions (less than 100 μm diameter, 0.1 mm). Microanalytical techniques must be used. On examining a range of samples using FTIR microscopy, the inclusions were found to comprise lead carboxylates (lead fatty acid soaps) and lead carbonate. The distribution of the components in the inclusions was investigated in more detail for a sample of lead-tin yellow paint from Lorenzo Costa's *A Concert* (National Gallery No. NG 2486, dated ca. 1485-95), which has relatively large inclusions (Fig. 1). As is typical, the inclusions have a fairly opaque centre with a more translucent halo that fluoresces in UV light. Further details of the analysis of this paint sample, and other samples demonstrating this phenomenon, are given in reference [1]. Although the IR bands for lead carboxylates and lead carbonates overlap in the 1400 cm^{-1} region, the ratio of the peaks at 1400 and 1500 cm^{-1} indicates that the halos are rich in lead fatty acid soaps (Fig. 2, upper trace) and that the more opaque centres of the inclusions are rich in lead carbonate (Fig. 2, lower trace). Bands at 3535, 1400, 1045 and 682 cm^{-1} demonstrate that the lead carbonate in the Costa painting is present in the hydrocerussite form, $2PbCO_3 \cdot Pb(OH)_2$. Fig. 3 shows the spectrum of hydrocerussite. The higher lead density in the core of the inclusion (where there is lead carbonate rather than lead

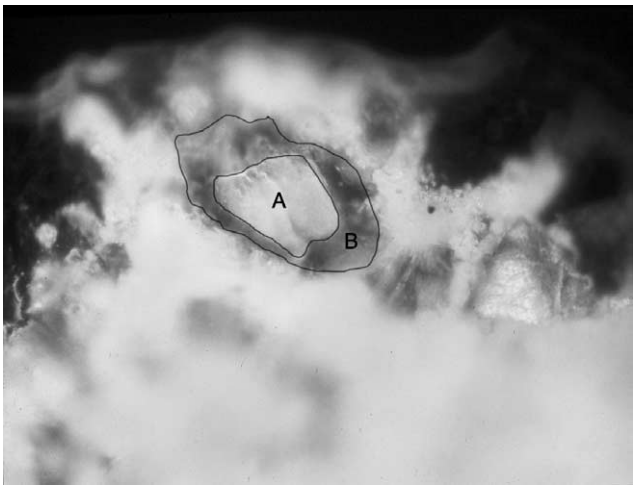

Fig. 1. Lorenzo Costa, *A Concert* (NG 2486), ca. 1485–95. Unmounted paint fragment from a lead-tin yellow highlight on the brocade of the woman's sleeve. One inclusion is outlined, and a translucent 'halo' (marked 'B') can be seen around a more opaque core (marked 'A').

carboxylates) is confirmed by examination of the back-scattered image (BSI) in the scanning electron microscope. In the BSI, the centre of the inclusion is more highly scattering (i.e., lead rich) than the surrounding halo.

Occasionally, as is seen for a sample from a lead-tin yellow highlight in *The Avenue at Middleharnis* by Meindert Hobbema (NG 830, dated 1689), the inclusions contain less lead carbonate. This is reflected in their more homogeneous appearance in the BSI in the SEM (Fig. 4). Fig. 5 shows the IR spectrum of an inclusion from the Hobbema, and for comparison traces (ii) and (iii) show the spectra of lead palmitate and stearate, respectively. The strong, sharp bands at 2918 and 2849 cm^{-1} correspond to the C—H stretches of the fatty acid portion of the lead soaps. The asymmetric carboxylate stretch of the lead fatty acid soaps appears as a doublet at 1540 and 1513 cm^{-1} and the symmetric stretch at about 1419 cm^{-1}. The pattern of small peaks in the 1350–1180 cm^{-1} region corresponds to the vibrations associated with the long hydrocarbon chains of the fatty acids.

GC-MS analysis of the total fatty acid content of a typical aged drying oil paint film suggests that just three acids comprise the bulk of the monomeric content – palmitic, stearic and azelaic acids [1,9]. Fig. 6 shows the IR spectrum of the dicarboxylate salt, lead azelate. The fingerprint region is very different to that for the monocarboxylate salts (see Fig. 5), thus allowing lead palmitate or stearate to be distinguished from lead azelate when pure. In the presence of the oil medium and

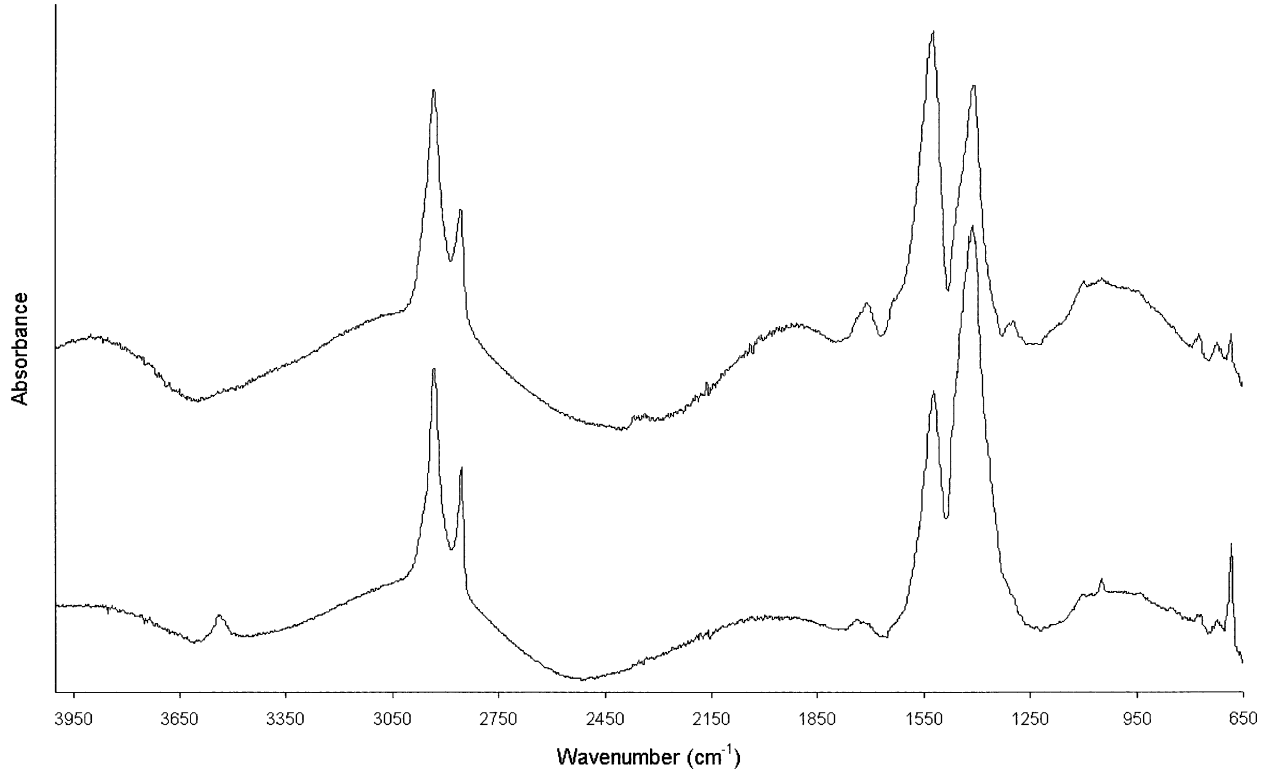

Fig. 2. Lorenzo Costa, *A Concert*. FTIR spectra (4000–650 cm^{-1}) from the inclusion illustrated in Fig. 1. Upper trace: spectrum from the translucent 'halo' around the inclusion (marked 'B' in Fig. 1), which has a high proportion of lead-fatty acid soaps. Lower trace: spectrum from the more opaque centre of the inclusion (marked 'A' in Fig. 1), which has a high proportion of lead carbonate. (The baseline roll in the spectra is an artefact resulting from the use of a diamond cell in sample preparation.)

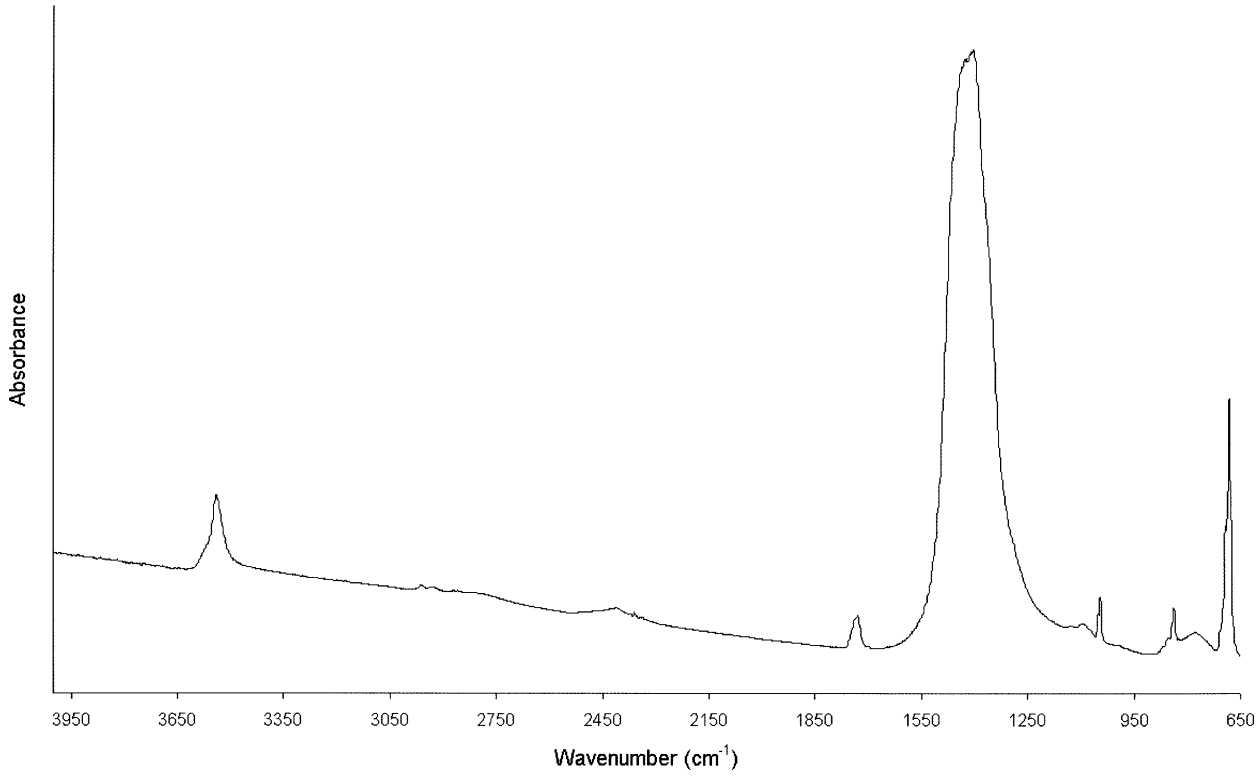

Fig. 3. FTIR spectrum (4000–650 cm^{-1}) of lead white ($2PbCO_3 \cdot Pb(OH)_2$, hydrocerrusite).

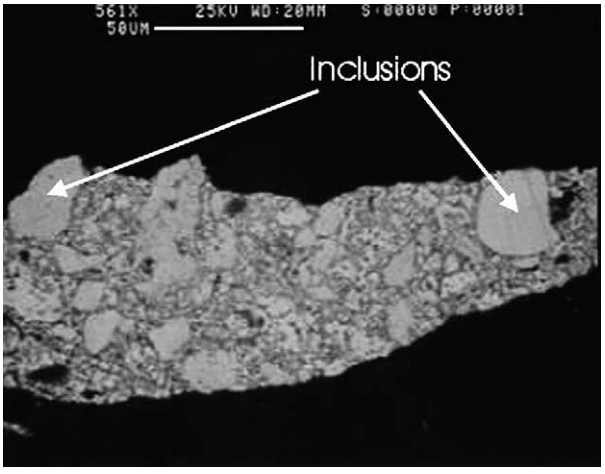

Fig. 4. Meindert Hobbema, *The Avenue at Middelharnis* (NG 830), 1689. Back-scattered electron image of a paint cross-section from the lead-tin yellow highlight of the small tree in sunlight. Two large inclusions are marked.

lead pigments, it can be difficult to tell by IR alone precisely which soaps are present in an inclusion. However, in the IR spectrum from the Hobbema (Fig. 5, upper trace) the absence of lead azelate is clear and the inclusion can be seen to consist of a mixture of lead palmitate and stearate. Indeed, if the fine structure in the IR spectrum in the 1360–1150 cm^{-1} region is examined in detail, it can be seen that the Hobbema trace (upper trace) is a combination of the palmitate (middle) and stearate (lower) traces. This result is confirmed by GC-MS analysis in cases where it has proved possible to isolate inclusions from the bulk paint matrix.

The Hobbema example, where very clear IR spectra are obtained, is not an isolated case. Equally well-resolved spectra have been obtained from inclusions in Karel Dujardin, *Portrait of a Young Man* (*Self Portrait?*) (NG 1680), ca. 1655 [1]. Inclusions were found both in layers containing red lead (an underpaint layer) and lead-tin yellow (a yellow highlight). Again, the inclusions could be seen to consist of a mixture of lead palmitate and stearate, but no lead azelate.

It is not known precisely how the lead soap protrusions form in the paint. Lead soaps are known to form on reaction of certain lead-based pigments with fatty acids in an oil medium [25], but what is less clear is why agglomerations of soaps form in the film, and how quickly this occurs. Slow migration of material through the paint film must be involved, perhaps driven by the changes that occur as the film ages. As a drying oil paint film ages the degree of cross-linking increases, and as oxygen becomes incorporated into the film and degradation reactions occur, the polarity increases [9]. Thus, pustule formation might be linked to the increasing incompatibility between the oil matrix and more mobile components such as free fatty acids and lead carboxylates. The absence of lead azelate in the agglomerations

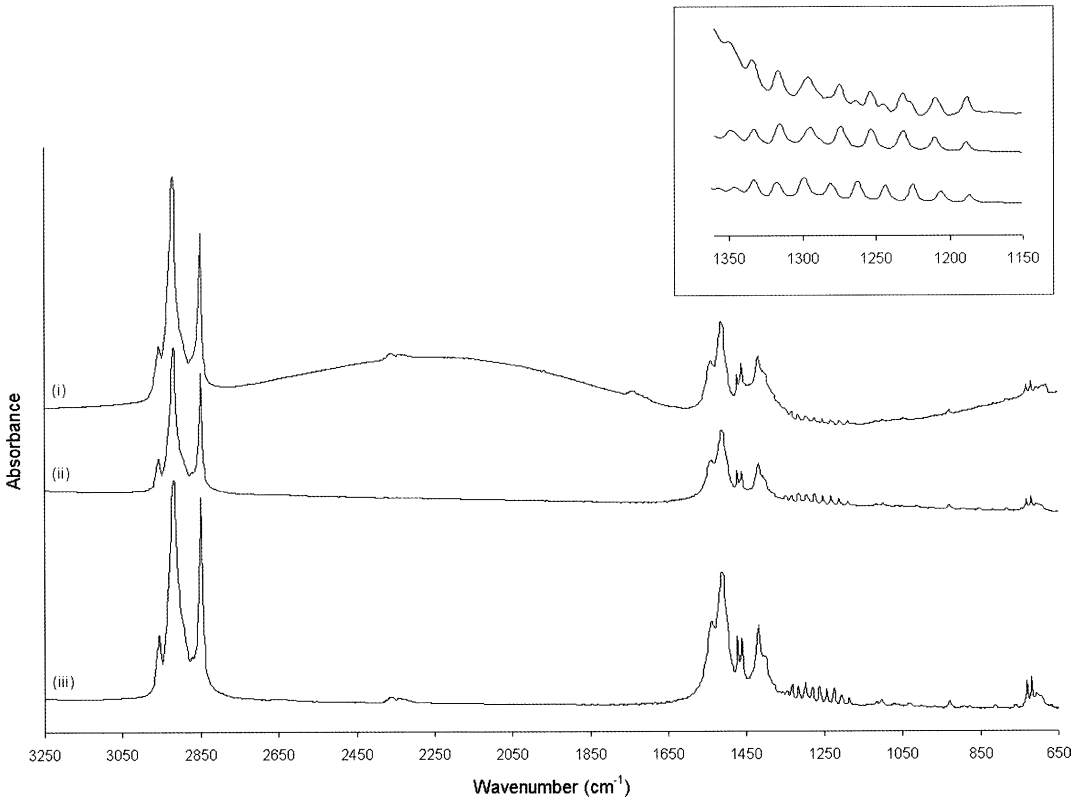

Fig. 5. FTIR spectra (3250–650 cm^{-1}) of: (i) an inclusion in the lead-tin yellow highlight on a tree from Hobbema, *The Avenue at Middelharnis* [upper trace]; (ii) a standard sample of lead palmitate [middle trace]; (iii) a standard sample of lead stearate [lower trace]. Inset: detail in the 1360–1150 cm^{-1} region of the FTIR spectra – order of traces as for main figure. (The baseline roll in the upper trace is an artefact resulting from the use of a diamond cell in sample preparation.)

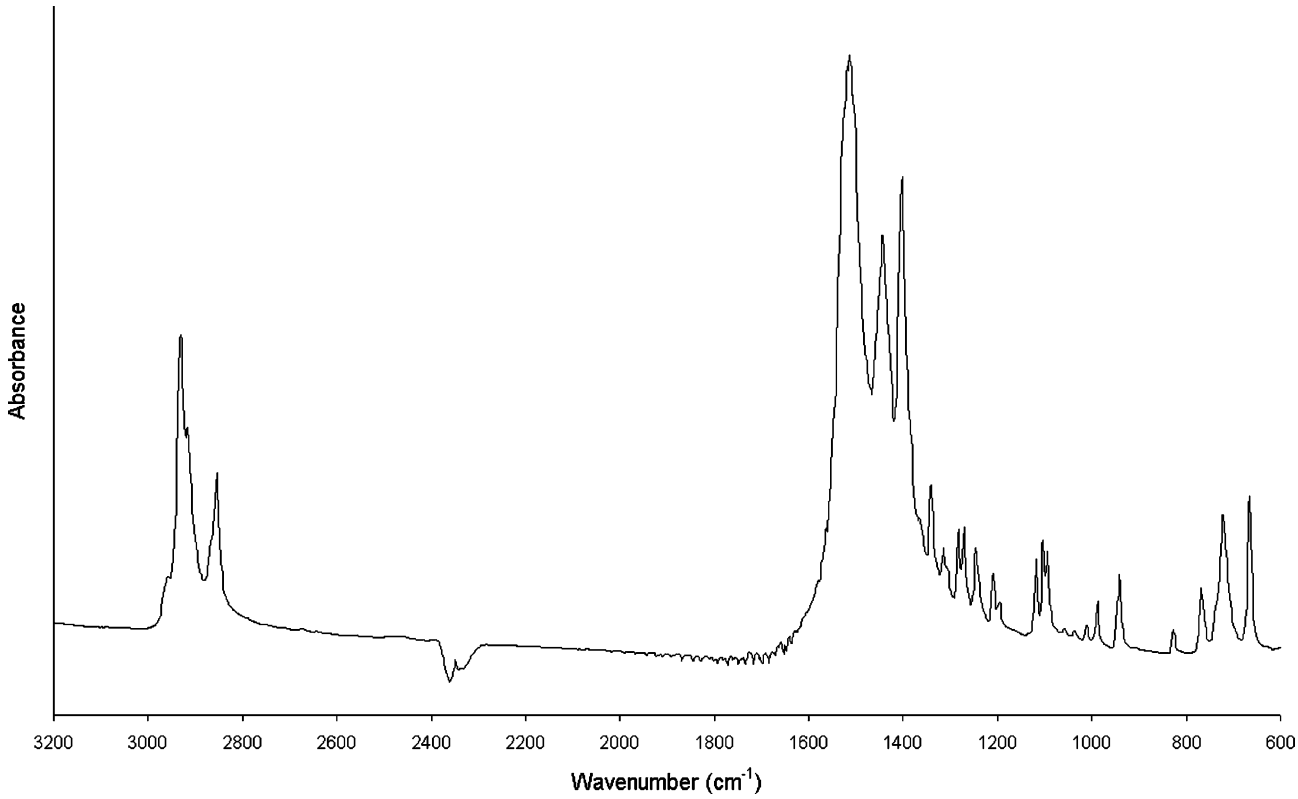

Fig. 6. FTIR spectrum (3200–600 cm^{-1}) of a standard sample of lead azelate.

suggests that the mobility of the fatty acid component is important. The higher polarity of azelaic acid and its lead salt, resulting from the shorter hydrocarbon chain and the two carboxylic acid groups, will make these components much less mobile than the monocarboxylic fatty acids. Further, the incorporation of the dicarboxylates into the ordered lamellar structure that is likely to exist in regions containing lead palmitate and stearate soaps is likely to be unfavourable. The mechanism evidently leads to the growth of lead soaps from more mobile fatty acids which has in many cases led to distortion of the surrounding paint layers and the appearance of blister-like protrusions at the paint surface. The formation of protrusions is probably dependent upon the comparatively low coverage, low number or clustering of nucleation sites which then leads to the growth of lead soaps. There may be a low coverage of nucleation sites owing to the flexible long chain fatty acids that will have to orientate, because there is a mixture of two of them and because the film will also contain other components and is therefore impure. However once nucleation has occurred, just like crystal growth, lead soap formation can proceed drawing in surrounding fatty acids by diffusion. Growth of the lead soap creates a lump particularly owing to the bulk of the hydrocarbon chains. Its growth must be energetically favourable. Conversion of the fatty acid group into a lead carboxylate anion is a thermodynamically favoured process. Packing or ordering of the hydrocarbon chains in the anticipated lamellar structure may also be an important driving process.

3.2. Crystal structure of lead(II) azelate

Bond lengths and angles are given in Table 1. Table 2 contains a summary of the key crystallographic data. The structure of the azelate ligand is shown in Fig. 7. The crystal structure of lead(II) azelate consists of a three-dimensional polymeric framework based on $(PbO_4)_n$ layers (Fig. 8) parallel to the crystallographic *a* and *b* axes. Adjacent layers are connected by nC$(CH_2)_7$C chains. These chains extend parallel to the *c* axis. This three-dimensional polymeric structure is depicted in Fig. 9. Fig. 10 shows the coordination of Pb.

Table 2
Summary of key crystallographic data for lead(II) azelate

Compound	
Empirical formula	$C_9H_{14}O_4Pb$
Formula weight	393.39
Temperature (K)	120(2)
Crystal system	monoclinic
Space group	$P2_1/m$
Unit cell dimensions	
a (Å)	4.7455(3)
b (Å)	7.1913(5)
c (Å)	14.7694(13)
α (°)	
β (°)	91.814(3)
γ (°)	
V (Å^3)	503.77(6)
Z	2
D_{calc} (Mg m^{-3})	2.593
Absorption coefficient (mm^{-1})	16.731
Crystal	block; colourless
Crystal size (mm)	0.15 × 0.15 × 0.04
θ range for data collection	3.15°–25.04°
Reflections collected [R_{int}]	2678 [R_{int} = 0.0360]
Independent reflections	964
Completeness to θ = 25.04°	98.7%
Data/restraints/parameters	964/72/84
Goodness-of-fit on F^2	0.959
Final *R* indices [$F^2 > 2\sigma(F^2)$]	$R1 = 0.0265$, $wR2 = 0.0626$
R indices (all data)	$R1 = 0.0291$, $wR2 = 0.0639$
Largest diffraction peak and hole (e Å^{-3})	1.806 and −1.174

Table 1
Bond lengths (Å) and angles (°)

Pb1—O2	2.382(9)	O2—Pb1—O3^{iv}	124.3(2)
Pb1—O1	2.453(7)	O1—Pb1—O3^{iv}	77.1(2)
Pb1—O3^{i}	2.543(6)	O3^{i}—Pb1—O3^{iv}	115.64(14)
Pb1—O3^{ii}	2.543(6)	O3^{ii}—Pb1—O3^{iv}	68.63(18)
O3—C9	1.243(7)	O3^{iii}—Pb1—O3^{iv}	47.5(2)
Pb1—O3^{iv}	2.677(5)	O2—Pb1—O1^{v}	74.0(2)
Pb1—O1^{v}	2.868(7)	O1—Pb1—O1^{v}	126.1(3)
O1—C1	1.247(12)	O3^{i}—Pb1—O1^{v}	90.89(11)
O2—C1	1.202(11)	O3^{ii}—Pb1—O1^{v}	90.89(11)
O2—Pb1—O1	52.1(2)	O3^{ii}—Pb1—O3^{iii}	115.64(14)
O2—Pb1—O3^{i}	82.59(16)	O3^{iii}—Pb1—O1^{v}	148.13(16)
O1—Pb1—O3^{i}	83.03(15)	O3^{iv}—Pb1—O1^{v}	148.13(16)
O2—Pb1—O3^{ii}	82.59(16)	C1—O1—Pb1	91.5(6)
O1—Pb1—O3^{ii}	83.03(15)	C1—O2—Pb1	96.1(7)
O3^{i}—Pb1—O3^{ii}	164.0(3)	C9—O3—Pb1^{i}	152.3(5)
O2—Pb1—O3^{iii}	124.3(2)	C9—O3—Pb1^{vi}	96.0(4)
O1—Pb1—O3^{iii}	77.1(2)	Pb1^{i}—O3—Pb1^{vi}	111.37(18)
O3^{i}—Pb1—O3^{iii}	68.63(19)		

Symmetry operators: (i) $-x, -y, -z$, (ii) $-x, y+1/2, -z$, (iii) $x, y, z+1$, (iv) $x, -y+1/2, z+1$, (v) $x+1, y, z$, (vi) $x, y, z-1$.

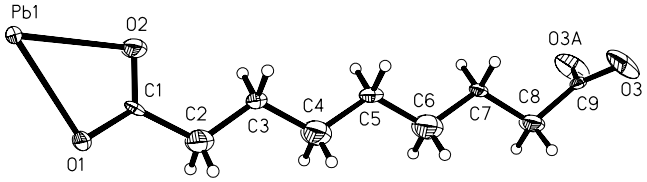

Fig. 7. The asymmetric unit in the structure of lead(II) azelate.

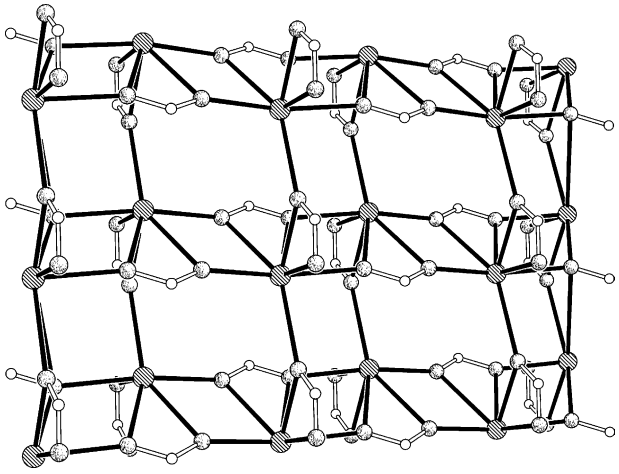

Fig. 8. The two-dimensional $(PbO_4C_2)_n$ core of the lead(II) azelate framework (solid bonds: Pb—O, open bonds: O—C).

Each Pb atom is coordinated by two chelating azelate ligands, one symmetrically and one asymmetrically bonded. Each oxygen atom of the symmetrically bonded azelate (O3) is coordinated to another Pb atom. Pb is additionally connected to one oxygen atom of the asymmetrically bonded azelate (O1) which is also coordinated to another Pb atom, thus forming the two-dimensional polymeric $(PbO_4)_n$ units. However, if only the coordination of Pb by the symmetrical azelate ligand is considered, the polymeric structure is just that of a $(PbO_2)_n$ chain parallel to the *b*-axis (Fig. 9(b)). This particular detail in the structure of lead(II) azelate is present also in the structures of lead(II) acetate trihydrate [26], lead(II) crotonate [27] and bis(*p*-amino-benzoato)lead(II) [28]. All these structures have a different

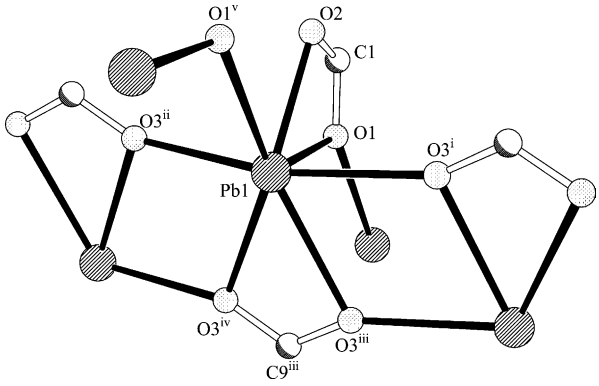

Fig. 10. The 7-fold coordination of Pb in lead(II) azelate. See Table 1 for symmetry operators.

space group. The $(PbO_2)_n$ chains propagate parallel to the *b*-axis in all cases, and the fact that the observed axial lengths for *b* are very similar within this group (Table 3) is just the result of this common structural feature.

All non-hydrogen atoms except O3 lie in a mirror plane. Two pairs of O3 oxygen atoms bridge between adjacent metal centres to give planar Pb_2O_2 rings with Pb—O distances of 2.543(6) and 2.677(5) Å. The Pb atom is displaced 0.326(6) Å from the plane formed by the four coordinating O3, in the direction of the apical azelate (O1 and O2). $O1^V$ *deviates* from this plane by 1.74(2) Å in *the* direction of the vacant coordination site. The Pb—$O1^V$ bond length of 2.868(7) Å is considerably longer than both apical Pb—O bonds. Here, the bond to the non-bridging O2 atom 2.382(9) Å is the shortest. The

Table 3
Crystallographic details for polymeric $(PbO_2C)_n$ chains similar to that shown in Fig. 9(b)

Compound	Space group	Direction	Vector length (Å)	Ref.
Lead(II) azelate	$P2_1/m$	[0 1 0]	7.191	[this work]
Lead(II) acetate trihydrate	$C2/m$	[0 1 0]	7.269	[26]
Lead(II) crotonate	$P\bar{1}$	[0 1 0]	7.339	[27]
Bis(*p*-aminobenzoato)lead(II)	$P2_1/c$	[0 1 0]	7.505	[28]

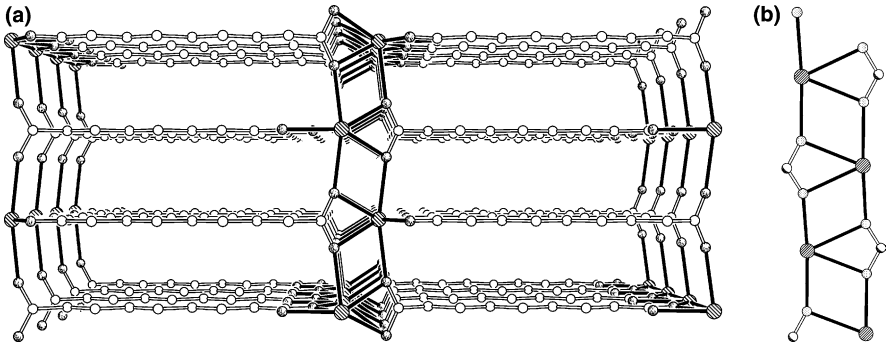

Fig. 9. (a) The polymeric structure of lead(II) azelate (solid bonds: Pb—O, open bonds: O—C, C—C). View along the *a*-axis. (b) Detail of (a). $(PbO_2C)_n$ chain.

closest Pb···O non-bonded contacts are 3.703(7) Å to O3 $(x+1, y, z)$ and O3 $(-x+1, 1/2-y, z)$.

The Pb1—O1—C1—O2 chelate ring that lies in a mirror plane with the azelate carbon atoms is subsequently perfectly planar, whereas considerable deviation from planarity is shown by the second chelate ring, Pb1—O3—C9—O3^{i}. The distance between C9 and the PbO_2 plane is 0.41(1) Å. The mean planes of two chelate rings belonging to the same azelate moiety form an angle of exactly 90.0°.

4. Conclusions

Analysis using FTIR spectroscopy of the inclusions found in microscopic oil paint samples from works in the National Gallery's collection has shown that lead fatty acid soaps are present. In some cases pure lead soaps have been observed directly. Only lead palmitate and stearate are found, but no lead azelate is present. Lead azelate can readily be prepared and has been fully characterised. It is postulated that its absence from inclusions within the paint film is linked to the higher mobility of lead monocarboxylates within an aged oil paint film. Protrusion formation is thought to be dependent upon the comparatively low coverage, low number or clustering of nucleation sites in the film.

5. Supplementary material

Crystallographic data have been deposited with the Cambridge Crystallographic Data Centre as supplementary publication no. CCDC 209611. Copies of this information may be obtained free of charge from the Director, CCDC, 12 Union Road, Cambridge, CB2 1EZ, UK (fax: +44-1223-336033; e mail: deposit@ccdc.cam.ac.uk or www: http://www.ccdc.cam.ac.uk).

Acknowledgements

We are grateful to the EPSRC National Crystallography Service, University of Southampton and to Marika Spring from the National Gallery, Trafalgar Square, London.

References

[1] C. Higgitt, M. Spring, D. Saunders, Pigment–medium interactions in oil paint films containing red lead or lead-tin yellow, National Gallery Technical Bulletin, vol. 24, National Gallery Company, London, 2003 (in press).
[2] (a) R.M.A. Heeren, J.J. Boon, P. Noble, J. Wadum, in: J. Bridgland (Ed.), 12th Triennial Meeting Lyon, ICOM Committee for Conservation Preprints, James and James, London, 1999, p. 228;
(b) J. van der Weerd, J.J. Boon, M. Geldof, R.M.A. Heeren, P. Noble, Zeitschrift fur Kunsttechnologie und Konservierung 16 (2002) 36;
(c) J. van der Weerd, Ph.D. Thesis, FOM Institute for Atomic and Molecular Physics, Amsterdam, 2002.
[3] (a) M.-C. Corbeil, L. Robinet, Powder Diffr. 17 (2002) 52;
(b) L. Robinet, M.-C. Corbeil, Stud. Conserv. 48 (2003) 23.
[4] M.S. Akanni, E.K. Okoh, H.D. Burrows, H.A. Ellis, Thermochim. Acta 208 (1991) 1.
[5] (a) E.J. Dunn Jr., in: T.C. Patton (Ed.), Red Lead, Pigment Handbook, Properties and Economics, vol. 1, Wiley–Interscience, New York, 1973, p. 837;
(b) J.E.O. Mayne, in: T.C. Patton (Ed.), Pigment Electrochemistry, Pigment Handbook, Characterisation and Physical Relationships, vol. 3, Wiley–Interscience, New York, 1973, p. 457.
[6] E. Rocca, J. Steinmetz, Corros. Sci. 43 (2001) 891.
[7] J.-M. Rueff, N. Masciocchi, P. Rabu, A. Sironi, A. Skoulios, Chem. Eur. J. 8 (2002) 1813.
[8] J.-M. Rueff, N. Masciocchi, P. Rabu, A. Sironi, A. Skoulios, Eur. J. Inorg. Chem. 11 (2001) 2843.
[9] J.S. Mills, R. White, The Organic Chemistry of Museum Objects, second ed., Butterworths, London, 1994, 33 and 171.
[10] M.R.St.J. Foreman, M.J. Plater, J.M.S. Skakle, J. Chem. Soc., Dalton Trans. (2001) 1897.
[11] Lacouture, M. Francois, C. Didierjean, J.P. Rivera, E. Rocca, J. Steinmetz, Acta Crystallogr., Sect. C. 57 (2001) 530.
[12] G. Feio, H.D. Burrows, C.F.G.C. Geraldes, T.J.T. Pinheiro, Liq. Crystals 9 (1991) 417.
[13] M.A. Mesubi, J. Mol. Struct. 81 (1982) 61.
[14] M.R.St.J. Foreman, T. Gelbrich, M.B. Hursthouse, M.J. Plater, Inorg. Chem. Commun. 13 (2000) 234.
[15] M.J. Plater, M.R.St.J. Foreman, E. Coronado, C.J. Gómez-García, A.M.Z. Slawin, J. Chem. Soc., Dalton Trans. (1999) 4209.
[16] R. White, J. Pilc, in: The Application of FTIR-Microscopy to the Analysis of Paint Binders in Easel Paintings, National Gallery Technical Bulletin, vol. 16, National Gallery Company, London, 1995, p. 73.
[17] J. MacGee, K.G. Allen, J. Chromatogr. 100 (1974) 35.
[18] R.C. Mehrotra, R. Bohra, Metal Carboxylates, Academic Press, London, 1983 (Chapter 2).
[19] R.C. Weast (Ed.), Handbook of Chemistry and Physics, 68th ed., CRC Press, Boca Raton, 1987, p. B-100.
[20] A.M. Duisenberg, DIRAX, J. Appl. Cryst. 25 (1992) 92.
[21] R. Hooft, B.V. Nonius, COLLECT: data collection software, 1998.
[22] (a) R.H. Blessing, SORTAV, Acta Cryst. A 51 (1995) 33;
(b) R.H. Blessing, J. Appl. Cryst. 30 (1997) 421.
[23] P.T. Beurskens, G. Beurskens, W.P. Bosman, R. de Gelder, S. Garcia-Granda, R.O. Gould, R. Israël, J.M.M. Smits, DIRDIF-96, Crystallography Laboratory, University of Nijmegen, The Netherlands, 1996.
[24] G.M. Sheldrick, SHELXL97, University of Göttingen, Germany, 1997.
[25] E.J. Dunn Jr., in: R.R. Myers, J.S. Long (Eds.), Lead Pigments, Treatise on Coatings, Pigments, Part 1, vol. 3, Marcel Dekker, New York, 1975, p. 403.
[26] R.G. Bryant, V.P. Chacko, M.C. Etter, Inorg. Chem. 23 (1984) 3580.
[27] W. Clegg, I.R. Little, B.P. Straughan, Acta. Cryst. C 42 (1986) 1319.
[28] I.R. Amiraslanov, N.Kh. Dzhafarov, G.N. Nadzhafov, Kh.S. Mamedov, E.M. Movsumov, B.T. Usubaliev, Zh. Strukt. Khim. 21 (1980) 131.